

RSC Advances



This is an *Accepted Manuscript*, which has been through the Royal Society of Chemistry peer review process and has been accepted for publication.

Accepted Manuscripts are published online shortly after acceptance, before technical editing, formatting and proof reading. Using this free service, authors can make their results available to the community, in citable form, before we publish the edited article. This *Accepted Manuscript* will be replaced by the edited, formatted and paginated article as soon as this is available.

You can find more information about *Accepted Manuscripts* in the [Information for Authors](#).

Please note that technical editing may introduce minor changes to the text and/or graphics, which may alter content. The journal's standard [Terms & Conditions](#) and the [Ethical guidelines](#) still apply. In no event shall the Royal Society of Chemistry be held responsible for any errors or omissions in this *Accepted Manuscript* or any consequences arising from the use of any information it contains.

Continuous biocatalytic recovery of neodymium and europium

Angela J. Murray, Sarah Singh, Dimitrios Vavlekas, Mark R. Tolley,

Lynne E. Macaskie

Unit of Functional Bionanomaterials, Institute of Microbiology and Infection, School of Biosciences, University of Birmingham, Edgbaston, Birmingham, B15 2TT, United Kingdom.

Corresponding author:

Sarah Singh, Unit of Functional Bionanomaterials, Institute of Microbiology and Infection, School of Biosciences, University of Birmingham, Edgbaston, Birmingham, B15 2TT, United Kingdom. Contact no. 01214145434, email: s.singh.1@bham.ac.uk

Rare earth biorecovery as nanocrystallites

Abstract

Batch-grown cells and continuously-grown biofilm of a *Serratia* sp. were utilized to recover the rare earth elements (REEs) lanthanum and neodymium from solution. Selectivity was obtained for La(III) over Th(IV) using columns of polyacrylamide gel-immobilized cells challenged at a rapid flow rate, exploiting the different solution chemistries and behaviors of REEs(III) and Th(IV). Biofilm-grown cells had a ten-fold higher activity of the mediating phosphatase, which promotes metal deposition as the corresponding metal phosphate, reflected as a correspondingly enhanced level of removal of Nd(III) (as NdPO_4) in flow-through columns utilizing biofilm on reticulated foam. The biofilms retained activity in the removal of Nd(III) for > 1 year, losing activity exponentially with a half life of 3 months. The flow rate giving 50% removal ($\text{FA}_{1/2}$) of Nd(III) by 3 month old biofilms at pH 5.5 was 272 and 275 mL/h using two independent biofilm preparations, equivalent to a $\text{FA}_{1/2}$ of 34 column volumes/h for fresh biofilms. The removal of Nd(III) was sustained at pH down to 3.5 with approx. 20% of the column activity lost upon return to pH 5.5. A similar result occurred in the presence of the common REE leaching agent ammonium sulfate (100 mM), this did not affect the ability of *Serratia* sp. to recover REEs. With a view to the potential for future biomanufacturing of Nd(III)-catalyst, the deposited material was identified as NdPO_4 by X-ray powder diffraction with a nanoparticle size of 14.5 nm, irrespective of the biofilm age.

Key phrases: neodymium biorecovery, lanthanum biorecovery, selective rare earth biorecovery, continuous flow process, immobilized *Serratia* biofilm, nanocrystallite harvest.

Introduction

The platinum group metals (PGMs) are traditionally regarded as precious metals due to their scarcity, high price and, often, non-substitutability in catalysis. Working towards conservation of natural resources and 'clean' reprocessing, precious metals can now be biorecovered into nanoparticulate (NP), catalytically-active materials.¹⁻³ To meet the challenges of catalyst longevity and retention, the use of biofilm-immobilized bacterial cells stabilizes catalytic metallic NPs against attrition and loss, allowing continuous use.⁴ This technology is largely mature.

However, in contrast to the 'traditional' precious metals (i.e. the PGMs and gold), the rare earth elements (REEs) are emergent in this context. REEs have a number of essential, often unsubstitutable uses in modern applications, for example in magnets (i.e. Nd in permanent NdFeB magnets), electronics-based technologies, light-emitting applications (e.g. Eu) and in catalysis, for example, in 'cracking' (La, Nd, Sm), in chemical synthesis, e.g. in ethylene polymerization (Y), and in the rubber industry (Nd).⁵

Amongst the REEs, Nd is particularly interesting because of its specific use as a Ziegler/Natta catalyst for the production of isoprene and butadiene rubbers.⁵ Nd-based catalysts are favored over other lanthanides (Ln) as they are highly active and do not promote catalytic aging of the rubber.

In contrast to the PGMs, REEs are not scarce *per se* but their refining is complex and production is largely confined to China. This has led to increasing geopolitical issues regarding the supply and price of REEs in parallel with their strategic emergence. Although much research is being conducted on REEs, their beneficiation from ores and their recovery from wastes and scrap by existing methods requires significant chemical, gas or energy inputs and can generate large

quantities of waste products.⁶ In contrast, a biological method would be a new approach to REE recovery.

Like PGMs, REEs have not been generally regarded as having biological functions in nature; some were suggested but were poorly understood.⁷ The low biological availability of REEs under normal conditions has been suggested as a reason for their non-evolutionary development as components of metalloenzymes.⁸ However, where metal solubility would be more enhanced (e.g. in acidic waters), a role for lanthanides (Ln: La, Ce, Pr, Nd) has now been established in the extremely acidophilic methanotrophic bacterium *Methylacidiphilum fumariolicum* SolIV, reporting the purification of Ln(III)-containing methanol dehydrogenase.⁹ However, developing the metal binding motif of this enzyme for the biorecovery of REE would be difficult due to the low biomass yields of acidophilic methylotrophs. Also, once bound, the metal is held stably by coordination via multiple ligands⁹ such that its recovery would be difficult without sacrificing the protein and a single use capacity-limited recovery system would not be economic.

The goal of the present study is to show an enzymatically-based approach to the recovery of REEs based on established, readily scalable processes, with the expanded aim to recover REEs selectively against a background of Th(IV). This is because REEs occur commonly in primary ores of uranium and thorium; following solvent extraction of U for nuclear fuel, the residual Th remains as a persistent radioactive co-contaminant and a barrier to exploitation of many primary sources as well as to the valorization of tailings ponds containing substantial quantities of REEs.

Two biotechnological routes to REE biorecovery have been inspired from previous work on nuclear waste remediation, where the experimental use of trivalent actinides

(Am(III), Cm(III)) was mitigated, in part, by the use of REE(III) 'surrogates' for bioprocess development.

In the first approach, following a report that hydroxyapatite (HA) can take up Nd(III) and Dy(III) by substituting for Ca(II),¹⁰ Cm(III) was observed to sorb onto nanoscale enzymatically-made hydroxyapatite (bio-HA).¹¹ Using Eu(III), time-resolved laser fluorescence (TRLF), together with extended X-ray absorbance fine structure (EXAFS), identified the site of Eu(III) incorporation as into the grain boundaries, which are more numerous in the nanoscale ensembles of the many small crystallites which typify the biogenic material¹¹ as compared to its less effective commercial counterpart.¹² Re-dissolution of metals, once incorporated, was less using bio-HA than for commercial HA.¹³ Hence, while this may be a good approach for metal sequestration, there is a limit to the loading capacity; also, an alternative method would be preferred for easy recovery of REEs in forms suitable for onward refining or, indeed, for direct use as catalysts.

The manufacture of the bio-hydroxyapatite used for REE recovery was achieved via the well described acid phosphatase (PhoN) of an atypical *Serratia* sp. N14.^{14,15} Located within the periplasm, and also tethered within the extracellular polymeric material (EPM) matrix,¹⁶ this enzyme functions in resting and immobilized cells to liberate inorganic phosphate (Pi) and precipitate this with metallic ions to form well-defined metal phosphate biomineral deposits. In the case of Ca(II) the resulting mineral is bio-HA; corresponding minerals are formed with other metal ions. Hence, the method could be used for the direct biomineralization of REE phosphates.²

Early work established the utility of this direct enzymatic route for the removal of heavy metals as phosphates from acidic minewaters¹⁷ and nuclear waste;¹⁸ method development for the latter conveniently used a surrogate model whereby removal of

La(III) and Y(III) was shown,¹⁹⁻²¹ using polyacrylamide gel-immobilized cells in a continuous-flow process.²¹ More recently, the future potential of this approach was indicated for the continuous recovery of neodymium and europium.² More than 90% of the Nd(III) and 85 % of the Eu(III) was recovered from flows supplemented with 1 mM metal using a *Serratia* sp. biofilm immobilized on polyurethane reticulated foam at slow flow rates. However the capacity for metal removal at high flow rate, and biofilm-catalyst durability, were not established.

The choice of a biofilm for enzyme immobilization and hence stable metal fixation was validated previously. Natural biofilm of the phosphatase (PhoN)-bearing *Serratia* sp. was comparable in activity to planktonic cells chemically coupled to a solid support.²² Biofilm formation, extensively described in the literature,²³ is often mediated via specific adhesin molecules²⁴⁻²⁶ as well as via extensive adhesive extracellular polymeric material (EPM). Yong *et al.*²⁷ proved the utility of the natural *Serratia* biofilm to retain phosphate biomineral once deposited, the adhesion strength being, for fresh and HA-mineralized biofilm respectively, 3.4 and 126 J/m² (work done to detach biofilm from support). The metal phosphate product can be recovered easily by scraping the surface or, for porous supports like polyurethane reticulated foam, by squeezing the foam.

The objectives of this study were to establish removal of La(III) against a background of Th(IV), to establish the biofilm-catalyst as a durable method to recover REE from solution, to quantify this in terms of the flow rate sustained by columns containing immobilized biofilm, and to establish the stability of this function during storage of the biofilm at 4°C. For REE recovery from primary or secondary sources it is anticipated that a primary leaching step to solubilize the metals will be required for production of a liquor. Hence, the ability of the enzyme to function in the

presence of common leaching ligands was evaluated, following early work that showed robustness of the system against an excess of nitrate or sulfate ion.^{28,29}

In general chemical catalysis is optimal using nanoscale materials, where stabilization of nanoparticles against agglomeration is problematic, as well as scalability of their manufacture. The final aim of this study was to characterize the putative rare earth phosphate product with the wider goal of its biorefining from a waste source into a high value product.

Materials and Methods

Strains, media and bacterial growth

Serratia sp. NCIMB 40259 was used with permission of Isis Innovation, Oxford. For comparison with early work²¹ initial studies used cells grown in batch culture (3 g/L glycerol; 0.67 g/L glycerol 2-phosphate in minimal salts medium).²¹ Studies using biofilm were based on conditions known to promote phosphatase overexpression and production of cellular adhesins.²⁴ Cells were grown in an air-lift fermenter with minor modifications to a published method.^{14,15,22} The central dividing plate used in earlier studies was removed and biofilm supports (reticulated foam discs: 2 cm diameter; 0.5 cm height; a gift from Recticel, Belgium) were held suspended in threaded rows (each disc sideways-on to the flow) throughout the whole vessel lumen. The medium comprised Tris-HCl buffer, KCl, (NH₄)₃PO₄, (nitrogen and phosphorus source) MgSO₄·7H₂O and FeSO₄·7H₂O¹⁴ with the carbon source (lactose; to 0.6 g/L) added aseptically after autoclaving. Pre-growth was done from an agar plate into non carbon-limiting medium (3 g/L lactose; 2 days) followed by transfer to lactose-limiting medium (24h; inoculum 5 mL; total volume 100 mL) and

aseptic transfer into the chemostat vessel pre-filled with medium. The culture was grown batch-wise overnight and then transferred to continuous mode ($D = 0.1^{14}$) for 6 days to allow biofilm development, with the outflow sent to waste after monitoring the pH and phosphatase activity.

The stringed biofilm-foam discs were withdrawn after 6 days, and then stored at 4 °C suspended over saline (8.5 g/L NaCl) in a closed vessel to maintain humidity. The biofilms were evaluated immediately or stored until use (3-12 months) without further treatment. As the foam discs were from different precise locations within the original vessel immobilized biofilm columns were made using an assortment of 8 discs taken from the same locations in the vertical aspect of the original string which was stored in the same orientation, in order to ensure that each column contained an equivalent mix of discs. Biofilms were prepared from two independent cultures (I and II) separated by one year.

Determination of phosphatase activity of the cells during growth

Phosphatase activity was monitored throughout biofilm growth by twice daily sampling from within the reactor, as well as using planktonic cells from the culture outflow, using the *p*-nitrophenyl phosphate (*p*NPP) assay (one unit of activity = nmol *p*-nitrophenol liberated/min/mg of bacterial protein).^{14,15,22}

Preparation of immobilized cell columns

For columns using polyacrylamide gel-(PAG) immobilized cells the immobilization was made using batch-pregrown cells and columns were prepared using shredded PAG as described by Tolley *et al.*²¹ Each column contained 1 g wet weight of cells

(100 mg dry weight) in a column of total volume of ~ 25 mL (the fluid volume was not determined).

For the biofilm-discs colonization throughout the foam was shown previously using magnetic resonance imaging (MRI ¹⁴) and the biofilm depth was estimated as up to ~ 400 μm by MRI ¹⁴ and by confocal laser scanning microscopy.²⁴ The diffusional depth of substrate and metal into the biofilm was not determined. Biofilm-reactors for metal uptake tests comprised glass columns (height: 5 cm, internal diameter: 2 cm, glass thickness 1.5 mm) each packed with 8 stacked biofilm-loaded discs. Using water displacement and foam discs without biofilm, the column fluid volume was determined as ~8 mL/column. The mass of a dry non-biofilm coated polyurethane disc was estimated from the average of 37 discs (mean 34.67 mg/disc) which was used to estimate the wet mass of biofilm for each set of 8 discs used per column (124 mg) by difference after drying the loaded discs to constant weight. This agrees with the value published previously (120 mg wet weight/column ³⁰), i.e. in this study ~12.4 mg dry weight/column (wet weight: dry weight mass/mass was 10:1) which was nominally ~ 7-8-fold less biomass than a PAG-column although no direct comparison is possible because the substrate and metal permeation throughout PAG and biofilm was not compared.

Challenge of the columns with rare earth elements and thorium and metal analysis

All glassware was cleaned by washing with Decon 90 (2%) and then HCl (~ 0.1 M) followed by 3 rinses with distilled water before use. The rare earth elements used in this study were lanthanum(III), neodymium(III) and europium(III). Stock solutions of 100 mM of metals were made using metal nitrate salts (Analar), which were then

diluted to 1 mM in final column solutions. The free metal concentration in solution was not measured in the presence of the organic complexing agents (below).

Stock solutions were as follows: tri-sodium sodium citrate (100 mM); citric acid (100 mM); glycerol 2-phosphate (100 mM) and metal solution (100 mM) (stored at 4 °C). These were diluted to final concentrations for use as: citrate buffer 2 mM (pH 5.5 or as described), glycerol 2-phosphate 5 mM and metal solution 1 mM (or as otherwise stated). Columns containing shredded polyacrylamide gel²¹ or 8 biofilm-coated discs were challenged (upflow; peristaltic pump) with the mixture adjusted to pH 5.5 (with HCl) or as described.

With each new solution to be tested, or at each new flow rate, a minimum of 2 column volumes (individual column capacity 8 mL.: 2 column volumes 16 mL) was allowed to pass through the column before samples were taken, in order to ensure solution displacement; plug flow behavior was shown previously by MRI.⁴ Metal removal was determined at various flow rates, presented as log values (Table 1).

Analysis of metals

For analysis of rare earth (RE) metals (La(III), Nd(III), Eu(III)) a spectrophotometric method using arsenazo III was used based on a method described by Fritz and Bradford.^{21,31} The arsenazo III reagent is sensitive but not selective. For determination of La(III) and Th(IV) in the presence of each other Th(IV) was extracted into dioctyl phenyl phosphonate (DOPP) in hexane (30:70 vol/vol) which, in the presence of 1.45 M HNO₃, gave 100% extraction of Th(IV) and no extraction of La(III) which remained in the aqueous layer.²⁰ The HNO₃ reduced the sensitivity of the reagent by ~ 75% (A_{652}); hence extracted samples (aq.) were brought to the initial pH value by addition of NaOH (160 mM)²⁰ and checked against La(III)

reference solutions without the extraction step. Pure metal solutions were analyzed by appropriate dilution into 2 mL in the appropriate 2 mM citrate/ 5 mM glycerol 2-phosphate mixture to which was added 0.3 mL of 0.75 M HCl and 0.1 mL of arsenazo III reagent.³¹ Mixed samples were estimated at A_{652} against a blank of the appropriate mixture. For a mixed Th(IV)/La(III) solution a divided solution was analyzed before (total Th(IV) + La(III)) and after (La(III) only) Th(IV) extraction into DOPP and the respective metal concentrations were estimated using simultaneous equations.²⁰

Estimation of phosphate release by the columns

The phosphate content of column outflows was measured using the molybdenum blue assay.³² To estimate total phosphate release the free inorganic phosphate in the column outflow was determined by assay and the total phosphate released was estimated by adding this value (P_i ; mM) to the phosphate accountable within the metal precipitate by metal assay (mM) (above) (assuming 1:1 metal and phosphate in the precipitate²¹ which was confirmed in this study: see later).

Scanning electron microscopy (SEM) and energy dispersive X-ray microanalysis (EDX)

An autoclaved disc free of biofilm was cut in half and gold-coated before being viewed on copper grids using a Phillips XL30 electron microscope at the School of Metallurgy and Materials, University of Birmingham, in comparison to a biofilm-coated disc that had undergone metal recovery for several weeks. Prior to SEM analysis discs with accumulated metal phosphate were stored in MOPS-NaOH buffer (20 mM, pH 7) and refrigerated. One half of a polyurethane disc, heavily loaded with

neodymium phosphate was washed in distilled water (by careful immersion) air-dried, gold sputter-coated and examined as above. For energy dispersive X-ray microanalysis (EDX) discs were cut into small (5 mm x 5 mm) sections prior to air-drying. The precipitate on the biofilm-polyurethane foam, as well as loose powder precipitate removed by squeezing, were analyzed by EDX using carbon coated samples (to ensure elements present were not masked by coating) prior to analysis and mounted onto to a copper grid.

X-ray powder diffraction analysis

Neodymium phosphate-loaded polyurethane discs were prepared as above and the retained halves were squeezed to release accumulated material. Washed samples (H_2O) were left overnight to air-dry; the powder was then analysed by XRD at the School of Chemistry, University of Birmingham, using a Bruker AXS D8 Diffractometer. Initially samples were examined between 5-70 degrees 2 theta, 0.02 degrees per step, scan time of 0.5 seconds per step, total scan period 30 minutes. A further analysis improved the diffraction pattern by focusing on a smaller range with data collected between 10 and 50 degrees 2 theta, 0.02 degrees per step, scan time of 1.6 seconds per step (total scan time of 1 hour). The acquired powder pattern was compared with the database standard powder pattern of NdPO_4 in the Joint Committee for Powder Diffraction Studies (JCPDS) database.

Results and Discussion

Phosphatase activity of the cultures and features of the PhoN phosphatase relevant to this investigation

The phosphatase activity of batch cultures was ~ ten fold less than that of the continuously-grown cells, being ~ 250 units (batch: Tolley *et al.* ²¹) and 236 ± 19 units (batch: Macaskie *et al.* ³³) (means of 2 and 20 experiments respectively) and ~2500 units (continuous culture: this study) in accordance with previous results.³⁴ The latter gave a specific activity of 2400 units in glycerol-limiting continuous culture with specific activities in batch culture varying from ~ 100-500 U depending on the degree of aeration.³⁴ The DO₂ in the chemostat (air lift fermenter) was not limiting *per se*, although the O₂ gradient within biofilms made within it was not measured. The PhoN phosphatase activity specifically represents the combined activity of two closely related isoenzymes which differ in some respects (e.g. charge, isoelectric point ³⁵) and the proportion of each of them varied according to the type of culture (batch or continuous) and also the DO₂.³⁴ From steady state chemostat-growth (glycerol-restriction) the extracted enzyme comprised approximately equal amounts of each isoenzyme;³⁴ the proportions in lactose-limited culture were not determined. Some degree of phosphotransferase activity (i.e. regeneration of glycerol-phosphate masking the absolute phosphoesterase activity) was not ruled out; glycerol 1-phosphate was shown in early work to be produced from added glycerol 2-phosphate using ³¹P NMR with similar results for the two isoenzymes;³⁶ glycerol 1-phosphate was not analyzed in the present work. Both enzymes were resistant to Cd²⁺, Zn²⁺ and Pb²⁺ but had similar sensitivities to UO₂²⁺ and Y³⁺ ($K_i \sim 30 \mu\text{M}$ ³⁷). In practice, in an active column rapid precipitation of metal phosphate will tend to prevent free metal ions from contacting the enzyme and inhibition is not observed as long as liberated phosphate is available to excess.

In vitro metal precipitation tests

A preliminary test was done *in vitro* in the column mixture (see Fig. 1) to establish the amount of phosphate needed to exceed the metal phosphate solubility product in this solution. Citrate was routinely incorporated to suppress metal hydrolysis but this would also reduce the amount of free metal ion in solution according to the metal-ligand dissociation constants.³⁸ The data show (Fig. 1) that La(III) phosphate precipitates at relatively low concentrations of phosphate (Pi). In contrast no precipitation of thorium phosphate was visible at up to 28 mM Pi. For comparison tests were also done with U(IV) which did not precipitate even with 44 mM Pi, although U(VI) required only 8 mM Pi (Fig 1). Early work indicated that the citrate complexing ability with respect to the trivalent ion is relatively low³⁹ and hence a restrictive complexation of the La(III) ion would require the use of strong complexing agents.⁴⁰ In contrast, for tetravalent ions, the binding to citrate is very strong³⁸ and hence the free concentration of metal available for precipitation is accordingly very low, resulting in poor precipitation even though M(IV) phosphate nominally has a very low solubility product. In practice, tetravalent metals do not occur as free M^{4+} ; without a chelating ligand they hydrolyze extensively. Hence, while Th-phosphate should form readily, the presence of Th(IV) predominantly as its citrate complex restricts its availability for precipitation according to the time taken to re-establish the equilibrium as each atom of Th(IV) is captured from solution into the precipitate. Importantly, these observations predict that if a time constraint is applied it should be possible to remove La(III) competitively against Th(IV), assuming that the rate of the dissociation of Th(IV) from its complex is slower than the flow residence time. This was tested as described below.

Removal of La(III) and Th(IV) by polyacrylamide gel-immobilized cells.

Previous work using flow-through columns showed that the flow rate giving 50% removal of La(III) ($FA_{1/2}$) was 300 mL/h and 480 mL/h for columns containing polyacrylamide gel-immobilized cells of phosphatase specific activity of 206 and 325 units, respectively (batch-grown cells; 100 mg cell dry weight per column). At flow rates of below ~180 mL/h complete removal of La(III) was observed.²¹ The effect of the low free concentration of Th(IV) in citrate (see above) as compared to La(III) was exploited to obtain La(III)-selectivity using columns at rapid flow rates. Here, nearly complete removal of La(III) was obtained but with negligible removal of Th(IV) (Fig. 2). Similar results were obtained for U(VI) but in this case only at the threshold flow rate at which complete La(III) removal started to be lost.²⁰ This agrees with the close desolubilization behavior of U(VI) and La(III) (Fig. 1) and achieving the correct balance could be problematic in operation. Mine wastes may contain relatively little U(VI) due to its prior removal but complete selectivity for REE(III) could be problematic in the case of leachates from primary ores. Here, bioreduction of U(VI) to U(IV) may be advantageous; this reaction has been well described in the literature.⁴¹

These studies show potential application of this biotechnology to the treatment of problematic mining wastes where the bulk of the U has been removed via solvent extraction for nuclear fuel but the separation of REEs from Th and residual U is an obstacle to commercial REE valorization from these sources. These data would underpin implementation of this approach against such wastes with the aim to valorise the REEs while leaving Th(IV). The latter could be removed for storage or diversion into thorium-based nuclear fuel cycles using a second column at the slow flow rate required for Th(IV) removal, with ammonium ion supplemented to promote formation of insoluble thorium ammonium phosphate.³²

The above study used 100 mg dry weight of cells of specific activity of ~ 250 units in a metal removing column of volume ~ 25 mL. The flow rate required to achieve 50% metal removal was proportional to the phosphatase specific activity.²¹ In order to increase the enzyme specific activity by ~ 10-fold (see above) continuously-grown cells were used in subsequent tests and employed as a biofilm, phosphatase and adhesin production being both upregulated by this method.²⁴ Polyacrylamide gel and reticulated foam are useful systems for small scale application but, at larger scale, additional mechanical strength is required; porous inorganic supports such as raschig rings have been shown as useful biofilm supports.²²

Table 2 compares PAG- and biofilm-immobilized cells normalized for the $FA_{1/2}$ value (the flow rate giving 50% removal of the metal) per mg cells for the removal of La(III)²¹ and Nd(III) (this study; see below). Assuming that La(III) and Nd(III) are removed comparably, this shows that the biofilm-system is superior by ~ 6-fold. However the biofilm data were acquired using biofilms that had been stored for 3 months, after which time ~ 50% of their activity has been lost (see below) and, correcting for this, it is apparent that the biofilm system is > 10-fold better in addition to not requiring costly or toxic immobilization precursors. Since the improvement by using biofilm was comparable to that which would be predicted from the enzyme specific activities (~ 10-fold: see above) these data also suggest that there are no major diffusional barriers although the biofilm substrate diffusional depth was not measured.

Use of biofilm-immobilized cells for REE recovery

For biofilm production early work used glycerol-grown cells in the chemostat but this occasionally produced an unstable culture, with selection of mutants with low

phosphatase activity (e.g. less than 100 units) over time.⁴² This could be overcome using a mutant which gave good biofilm in ~ 3-4 days⁴² but later work showed that a steady-state, reproducible phosphatase activity could be obtained by the substitution of lactose as the carbon source and this was routinely adopted in subsequent work.¹⁴ A further modification involved incorporation of an additional starter culture in the minimal medium which gave a reproducible phosphatase specific activity of ~ 2500 units. Biofilms from chemostat I were tested at 3, 7, 9, 10 and 12 months after storage at 4°C while biofilms from culture II were tested at the time of harvest and after 3 and 9 months.

The removal of Nd(III) and also Eu(III) (for comparison) for the two preparations is shown in Fig 3, using biofilms that had been allowed to age for 3 months. Here, a $FA_{1/2}$ value (that value giving 50% removal of the Nd(III), i.e. 0.5 mM) was obtained as 272 mL/h and 275 mL/h for the two preparations, showing 99% reproducibility between them.

Nd(III) and Eu(III) removal was similar with respect to the $FA_{1/2}$ value (Fig. 3) while other tests using PAG-immobilized cells showed that the removal of La(III) and Y(III) was, similarly, comparable.²⁰ Hence, this technique, although effective for rapid REE recovery against a background of Th(IV) (Fig 2) and also U(VI)²⁰ (not shown) does not select for one REE over another. The rapid production of a mixed metal phosphate concentrate into onward refining would represent a significant hydrometallurgical advance; however other studies have shown that refinements of this biotechnological approach can achieve some REE selectivity.⁴³ This approach, involving pre-nucleation of bacterial metal deposition sites with other metal phosphates, has the potential to be exploited to select for RE metal recovery from solution.⁴³ The same approach can be used to selectively block biorecovery of REEs,

presumably by competition for initial biosorption sites, resulting in enrichment of the excluded REE in the residual solution.⁴³ Such valorization would be highly valuable, indeed possibly mandatory, for future production of new catalysts from wastes; for example in contrast to Nd(III), Eu(III) catalyst has a low polymerization activity.⁵

The solution composition adopted in this study was the same as that described previously (5 mM glycerol 2-phosphate and 1 mM metal ion in 2 mM citrate buffer, pH 6.9²¹ or pH 5.5 (this study); the phosphatase activity was the same at both pH values using purified enzyme³⁵ or whole cells.²¹ The lower pH was selected for the work in this study since mine drainage waters tend to be acidic; preliminary studies showed that Nd(III)-accumulating columns were largely unaffected at pH values down to ~ pH 3.5⁴⁴ while uranium was removed from acid mine drainage waters.¹⁷

Analysis of the metal precipitate accumulated by the columns

Fig. 4a shows a reticulated foam disc without (inset) and with biofilm that had accumulated Nd(III) for several weeks, readily identified by the purple coloration (Fig. 4a). As suggested by Fig 4a the biofilm coverage was uneven with visible microcolonies, for example in the centre of the foam struts (Fig. 4b). Previous studies have shown that even in areas that appear uncolonized a monolayer layer of cells was visible.¹⁴ The appearance of the biofilm, overall, was similar at low resolution with and without metal (Fig. 4c,d). At higher resolution individual cells in the biofilm are visible (Fig. 4e) but these became completely obscured by the Nd-deposit after loading with Nd for several weeks (Fig 4f). The biofilm had a nodular appearance, with no individual cells visible (c.f. Fig. 4e; note that the magnification in Figs 4d and 4e was the same).

Mapping of an area of the metal-coated biofilm by EDX shows clearly the co-deposition of both Nd and P co-located with the organic material via carbon and oxygen mapping (Fig. 5a). Analysis of an area of the metal-biofilm by EDX (from the sample shown inset; Fig. 5b) shows clearly the co-deposition of Nd and P, with an elemental ratio (from atomic % calculation) of 1.01 ± 0.01 (mean \pm SEM; 6 samples, pooled data from cultures I and II) and hence the material was suggested to be NdPO_4 .

The putative identification of the precipitate as NdPO_4 was confined by X-ray powder diffraction, with the powder pattern indistinguishable from that of reference $\text{NdPO}_4 \cdot 2\text{H}_2\text{O}$ (Fig. 5c). However, despite the heavy loading of NdPO_4 and the complete occlusion of the cells by the precipitate (Fig. 4f), sharp diffraction peaks indicative of a crystalline material were not seen. This was in contrast to biogenic HUO_2PO_4 reported previously which was highly crystalline as evidenced by sharp peaks in the XRD powder pattern of HUO_2PO_4 produced by batch-grown cells.⁴⁵ It is possible (although it was not tested) that the presence of extensive EPM in biofilm-cells acts to prevent agglomeration of the crystals from multiple foci into large masses, which is very important if the material is to be used for further applications (e.g. catalysis) where nanoparticulate materials may give higher activity (due to their large surface area and reactive surface) than larger deposits. This also has implications with respect to the use of less aggressive leaching conditions if further metal purification is required downstream from biogenic metal phosphate. From Fig. 5c the crystallite size of the biogenic NdPO_4 was calculated by using the Scherrer equation as 14.8 nm and 14.5 nm from samples from the two independent preparations. Despite the reduction of metal-accumulating activity of the biofilm over time (see below) a biofilm that had been stored for 10 months at 4 °C before loading

with NdPO_4 gave a very similar X-ray powder pattern (not shown) to that shown in Fig. 5c.

Effect of storage on biofilm activity and metal removal

Fig. 6 shows the effect of storage time of the biofilm on the $\text{FA}_{1/2}$ value with respect to removal of Nd(III). The two independent cultures gave identical results when tested at the 3 month stage (see above) and for comparison the numerical values for $\text{FA}_{1/2}$ were normalized relative to 100%, with respect to the activity of fresh biofilm. Fig. 6 shows that biofilm activity was lost exponentially with time with a half life of ~ 3 months. This high stability is noteworthy since parallel experiments with the related organism *E. coli* showed that its biofilm detached from the support within a few weeks, along with a strong odor of decay.⁴⁶ Hence, although a recombinant strain of *E. coli* expressing PhoN and biomineralizing metal phosphate comparably to this *Serratia* sp.⁴⁷ would appear to have promise, the poor biofilm formation would restrict the applications of immobilized cells to those based on entrapment methods.

Tolerance of the biofilm to low pH and high salt concentration

For recovery of metals from slurries or solid scraps a method of leaching, usually at acidic pH, is required. Preliminary tests showed that at pH 3 the columns were inactivated irreversibly, showing no recovery when returned to the permissive pH. Fig. 7 shows the removal of neodymium at pH 5.5 and pH 3.5 in the standard column mixture. Following challenge at pH 3.5 metal removal was restored to ~ 80% of the original value on returning the column to pH 5.5. It is likely (but was not tested) that the fraction of enzyme activity lost was that contributed by the more labile isoenzyme (see earlier). The data of Fig. 7 are representative from two experiments with a

reproducibility between them of within 10% at pH 5.5. The $FA_{1/2}$ value at this pH was 38 mL/h, halving to 19 mL/h at pH 3.5 (with recovery to 30 mL/h when restored to pH 5.5). Hence, and as discussed with respect to uranium removal from acidic mine waters,¹⁷ the impact of operation at pH 3.5 is to reduce metal recovery by ~ 50% at a fixed flow rate, corresponding to a reduced phosphatase activity at low pH. In practice the flow rate can be reduced to accommodate the reduced activity. Since much of the activity is recovered on returning to pH 5.5 this suggests that the effect is mainly attributable to chemical factors, e.g. protonation of the substrate (with a resulting increased K_m), increased metal solubility at a lower pH (i.e. a reduced tendency to form a precipitate) or a combination of these factors.

A recent study⁴⁸ showed that, in contrast to noble metals, which require *aqua regia* for their solubilization from wastes, solubilization of more than 95% of the Y and Eu from fluorescent lamp wastes was achieved using 0.5 M HCl or HNO₃. However most studies on the leaching of REEs from substrates have focused on their recovery from natural materials such as ores^{49,50} or, more recently, clay minerals.^{51,52} Here, the leach solution was ammonium sulfate at 2% (0.15 M) and 0.05-2.5 M, respectively. A detailed examination⁵² showed that maximum Nd and Eu extraction (~ 85%) was achieved at 0.5 M (NH₄)₂SO₄ while at 0.1 M (NH₄)₂SO₄ the solubilization was reduced by only approx. 5% less than this value.

As a preliminary study to evaluate the potential to biorecover REEs from primary sources following (NH₄)SO₄ leaching, *Serratia* columns were supplemented with 0.1 M (NH₄)₂SO₄ sequentially at pH 5.5 and pH 3.5 and then returned to pH 5.5. The results with (NH₄)₂SO₄ at pH 5.5 were identical to those without it, (as shown in Fig 7). At pH 3.5 the $FA_{1/2}$ value with (NH₄)₂SO₄ was 17 mL/h and on return to pH 5.5 was 25 mL/h. Hence the ammonium sulfate had no marked effect on the degree of

recovery of the columns from the acidic pH. Importantly, these results show that, while 100 mM $(\text{NH}_4)_2\text{SO}_4$ achieves leaching from primary sources (see above) the ability of the immobilized cells to recover NdPO_4 is not compromised.

Ammonium sulfate precipitation is a standard method of protein preparation (salting-out). The phosphatase enzyme salts-out at 60% $(\text{NH}_4)_2\text{SO}_4$ ³⁵ and hence the concentration of $(\text{NH}_4)_2\text{SO}_4$ used was well below this threshold. It is concluded that this method of metal biorecovery has clear potential for the recovery of REEs from mineral and waste leachates (it was previously found effective against naturally leached solutions of UO_2^{2+} in mine waters¹⁷). However, as described above, many ores and mine wastes also contain Th(IV) and U(VI), whose mineralization as their phosphates is enhanced by ammonium ion.^{32,45} Hence, stringent preliminary evaluations will be needed in the choice of chemical leaching agent, to ensure that the results shown in Fig. 2 are not compromised in the presence of NH_4^+ that may be present in a leachate. For treatment of other liquid wastes it may be useful to first remove the REEs from solution and then supplement the solution with ammonium ion to biomineralize the U(VI) and Th(IV) using a second column. For a primary source that contains REEs, U and Th, the ammonium sulfate leaching method may reduce the selectivity (c.f. Fig. 2). In this case a mineral acid may be more beneficial; Yong and Macaskie^{28,29} showed the tolerance of the enzyme to nitrate and sulfate, while recent work showed that Nd-biomineralizing columns were largely unaffected by a ten-fold diluted solution of *aqua regia* at pH 3.5.⁴⁴ Current work aims to develop an optimal upstream leaching solution that retains downstream REE recovery with maximum selectivity. In this context the production of NdPO_x as nanocrystals (high surface area) has implications for applications of more benign leaching approaches

downstream, than those traditionally applied to RE phosphate ores such as monazite.

Metal removal has been described in terms of Michaelis-Menten kinetics with an additional 'inefficiency factor' which relates to the tendency of the metal to form a phosphate biomineral within the flow residence time.⁵³ This, in turn, relates to the relative concentrations of metal and phosphate (and the solubility product) and also to the presence of any complexing agents which may tend to reduce the free metal concentration (note that citrate was constant at 2-fold excess over the metal). Also, as the pH is reduced, the substrate glycerol 2-phosphate (as well as the citrate) will become protonated and hence the effect observed is a combination of any reduced substrate affinity (i.e. rise in apparent K_m) as well as, potentially, more free metal ion M^{3+} available for precipitation as the stability constant with citrate is pH-dependent. The flow rate-activity relationship is a combined result of all of these factors. In practice, therefore, the description of the column in this way enables an easy method to quantify the combined inhibitory effects of various factors as long as the reduction in metal removal is not due to irreversible enzyme damage. We show that the column system is robust at pH 3.5 and that the recovered material is pure $NdPO_4$ nanomaterial. Current studies are evaluating the scope for obtaining this from primary and secondary sources via leaching and biorecovery.

Conclusions

An enzymatically-mediated metal biorecovery method has been applied for the first time to the REEs neodymium and europium. Use of biofilm-immobilized bacteria allows a continuous recovery process which, by the choice of flow rate, facilitates

selective removal of REE(III) against Th(IV). The biorecovered NdPO₄ is in the form of nanocrystallites which has implications for onward use in catalytic applications.

Acknowledgements

We acknowledge with thanks the financial support of EPSRC and BBSRC, NERC ('Catalyst' award NE/K015664/1) and SERC for a studentship to MRT. We thank Dr Rich Boden (University of Plymouth, UK) for useful discussions and Recticel (Belgium) for the gift of reticulated foams.

References

1. L. E. Macaskie, I. P. Mikheenko, P. Yong, K. Deplanche, A. J. Murray, M. Paterson-Beedle, V. S. Coker, C. I. Pearce, R. Cutting, R. A. D. Patrick, D. Vaughan, G. van der Laan and J. R. Lloyd, in *Comprehensive Biotechnology*, ed. M. Moo-Young, M. Butler, C. Webb, A. Moreira, B. Grodzinski, Z. F. Cui and S. Agathos, Elsevier, Amsterdam, 2nd edn., 2011, vol. 6, pp. 719-725.
2. K. Deplanche, A. J. Murray, C. Mennan, S. Taylor and L. E. Macaskie, in *Nanomaterials*, ed. M. M. Rahman, Intech Publications, Rijeka, Croatia, 2011, ch. 12, pp. 279-314.
3. S. De Corte, T. Hennebel, B. de Gusseme, W. Verstraete and N. Boon, *Microb Biotechnol.*, 2012, **5**, 5-17.
4. D. A. Beauregard, P. Yong, L. E. Macaskie and M. L. Johns, *Biotechnol Bioeng.*, 2010, **107**, 11-20.
5. L. Friebe, O. Nuyken and W. Obrecht, in *Adv Polym Sci.*, ed. O. Nuyken, Springer Verlag, Berlin, 2006, **204**, pp. 1-154.

6. K. Binnemans, P. T. Jones, B. Blanpain, T. Van Gerven, Y. Yang, A. Walton and M. Buchert, *J Clean Prod.*, 2013, **51**, 1-22.
7. G. Tyler, *Plant Soil*, 2004, **267**, 191-206.
8. S. Lim and S. J. Franklin, *Cell Mol Life Sci.*, 2004, **61**, 2184-2188.
9. A. Pol, T. R. M. Barends, A. Dietl, A. F. Khadem, J. Eygenstein, M. S. M. Jetten and H. J. M. Op den Camp, *Environ Microbiol.*, 2014, **16**, 255-264.
10. E. I. Get'man, S. N. Loboda, T. V. Tkachenko, A. V. Ignatov and T. F. Zabirko, *Funct Mater.*, 2005, **12**, 6-10.
11. K. Holliday, S. Handley-Sidhu, K. Dardenne, J. C. Renshaw, L. E. Macaskie, C. Walther and T. Stumpf, *Langmuir*, 2012, **28**, 3845-3851.
12. S. Handley-Sidhu, J. C. Renshaw, S. Moriyama, K. Sasaki and L. E. Macaskie, *Environ Sci Technol.*, 2011, **45**, 6985-6990.
13. S. Handley-Sidhu, J. A. Hriljac, M. O. Cuthbert, J. C. Renshaw, R. A. D. Patrick, J. M. Charnock, B. Stolpe, J. R. Lead, S. Baker and L. E. Macaskie, *Environ Sci Technol.*, 2014, **48**, 6891-6898.
14. L. E. Macaskie, P. Yong, M. Paterson-Beedle, A. C. Thackray, P. M. Marquis, R. L. Sammons, K. P. Nott, and L. D. Hall, *J Biotechnol.*, 2005, **118**, 187-200.
15. M. Paterson-Beedle, K. P. Nott, L. E. Macaskie and L. D. Hall, *Methods Enzymol.*, 2010, **337**, 285-305.
16. B. C. Jeong, C. Hawes, K. M. Bonthron and L. E. Macaskie, *Microbiology*, 1997, **143**, 2497-2507.
17. L. E. Macaskie, P. Yong, T. C. Doyle, T. M. Manzano and M. Roig, *Biotechnol Bioeng.*, 1997, **53**, 100-109.
18. M. Paterson-Beedle and L. E. Macaskie, unpublished work.

19. L. Diels, L. E. Macaskie, M. Tsezos, T. Pumpel and F. Glombitza, Final Report EU contract BE-5350, 1995.
20. M. R. Tolley, Ph.D. Thesis, University of Oxford, 1993.
21. M. R. Tolley, L. S. Strachan and L. E. Macaskie, *J Ind Microbiol.*, 1995, **14**, 271-280.
22. J. A. Finlay, V. J. M. Allan, A. Conner and L. E. Macaskie, *Biotechnol Bioeng.*, 1999, **63**, 87-97.
23. T. Romeo, ed., in *Bacterial Biofilms. Current Topics in Microbiology and Immunology*, Springer-Verlag, Heidelberg, 2008, pp. 294.
24. V. J. M. Allan, M. E. Callow, L. E. Macaskie and M. Paterson-Beedle, *Microbiology*, 2002, **148**, 277-288.
25. W. Bokranz, X. Wang, H. Tschape and U. Romling, *J Med Microbiol.*, 2005, **54**, 1171-1182.
26. D. Linke and A. Goldman, eds., in *Bacterial Adhesion: Chemistry, Biology and Physics*, Springer Verlag, Berlin, 2011, vol. 715.
27. P. Yong, M. Paterson-Beedle, W. Liu, Z. Zhang, D. A. Beauregard, M. L. Johns and L. E. Macaskie, *Adv Mater Res.*, 2009, **71-73**, 741-744.
28. P. Yong and L. E. Macaskie, *Biotechnol Bioeng.*, 1997, **55**, 821-830.
29. P. Yong and L. E. Macaskie, *J Chem Technol Biotechnol.*, 1999, **74**, 1-8.
30. C. Mennan, M. Paterson-Beedle and L. E. Macaskie, *Biotechnol Lett.*, 2010, **32**, 1419-1427.
31. J. S. Fritz and E. C. Bradford, *Anal Chem.*, 1958, **30**, 1021-1022.
32. P. Yong and L. E. Macaskie, *J Chem Technol Biotechnol.*, 1995, **64**, 89-95.
33. L. E. Macaskie, J. D. Blackmore and R. M. Empsom, *FEMS Microbiol Lett.*, 1988, **55**, 157-162.

34. B. C. Jeong and L. E. Macaskie, *Enzyme Microb Technol.*, 1999, **24**, 218-224.
35. B. C. Jeong, P. Poole, A. C. Willis and L. E. Macaskie, *Arch Microbiol.*, 1998, **169**, 166-173.
36. B. C. Jeong, H. W. Kim and L. E. Macaskie, *FEMS Microbiol Lett.*, 1997, **147**, 103-108.
37. B. C. Jeong and L. E. Macaskie, *FEMS Microbiol Lett.*, 1995, **130**, 211-214.
38. L. D. Petit and K. J. Powell, Stability Constants Database. SC-Database IUPAC and Academic Software UK, 2008.
39. N. I. Udal'stova, in *Analytical Chemistry of uranium*, ed. A. P. Vinogradov, Ann- Arbor, London, 1970, pp. 5-27.
40. D. I. Ryabchikov and V. A. Ryabukhin, eds., in *Analytical chemistry of yttrium and the lanthanide elements*, Ann- Arbor, London, 1970, pp. 89-92.
41. R. T. Anderson and D. R. Lovley, in *Interactions of microorganisms with radionuclides*, ed. M. Keith-Roach and F. R. Livens, Elsevier, Amsterdam, 2002, vol. 2, ch. 7, pp. 205-223.
42. P. Clark, A. J. Butler and L. E. Macaskie, *Biotechnol Tech.*, 1990, **4**, 345-350.
43. A. J. Murray, S. Singh, D. Vavlekas, M. R. Tolley, T. P. Hathway, R. E. Baylis, R. Boden and L. E. Macaskie, presented in part at the 53rd Annual Conference of Metallurgists COM, Vancouver, September, 2014.
44. S. Singh and D. Vavlekas, unpublished work.
45. P. Yong and L. E. Macaskie, *J Chem Technol Biotechnol.*, 1995, **63**, 101-108.
46. C. Mennan and L.E. Macaskie, unpublished work.
47. G. Basnakova, E. Stephens, M. C. Thaller, G. Rossolini and L. E. Macaskie, *Appl Microbiol Biotechnol.*, 1998, **50**, 266-272.
48. C. Tunsu, C. Ekberg and T. Retegan, *Hydrometallurgy*, 2014, **144-145**, 91-98.

49. T. Jun, Y. Jingqun, C. Ruan, R. Guohua, J. Mintao and O. Kexian, *Hydrometallurgy*, 2010, **101**, 166-170.
50. T. Jun, Y. Jingqun, C. Kaihong, R. Guohua, J. Mintao and C. Ruan, *Hydrometallurgy*, 2010, **103**, 211-214.
51. G. A. Moldoveanu and V. G. Papangelakis, *Hydrometallurgy*, 2012, **117-118**, 71-78.
52. G. A. Moldoveanu and V. G. Papangelakis, *Hydrometallurgy*, 2013, **131-132**, 158-166.
53. L. E. Macaskie, R. M. Empson, F. Lin and M. R. Tolley, *J Chem Technol Biotechnol.*, 1995, **63**, 1-16.

Tables

Table 1 Solution flow rate through column showing how LnF (see X axis of Figures) derives from flow rate (F) mL/h

LnF (mL/h)	F (mL/h)
2.5	12.2
3.0	20.1
3.5	33.1
4.0	54.6
4.5	90.0
5.0	148.4
5.5	244.7
6.0	403.4

Table 2 Comparison of REE removal by polyacrylamide gel-immobilized and biofilm-columns

	PAG column	Biofilm column
Dry weight of cells	100 mg	12 mg
Column volume	25 mL	8 mL
FA _{1/2} for La(III) mL/h (Tolley <i>et al.</i> , 1995)	390 mL/h	-
FA _{1/2} per mg cells	3.9 mL/h	-
FA _{1/2} for Nd removal (this study; Fig. 3)	-	273.5 mL/h
FA _{1/2} per mg cells (determined at biofilm age 3 months)	-	22.8 mL/h
FA _{1/2} per mg cells (corrected for fresh biofilm (see text))	-	45.6 mL/h

Figure legends

Figure 1. Precipitation of U(VI), U(IV), Th(IV) and La(III) in cell-free test solution.

Metals were added as their nitrate salts to the column mixture (to 1 mM) and sodium phosphate solution was added (at the same pH) to the concentration shown (mM).

Tubes were mixed and examined after 10 and 30 min for visible precipitate. Black: precipitate visible in 10 min. Grey: precipitate visible in 30 min. White: no precipitate after 30 min.

Figure 2. Removal of La(III) and Th(IV) by polyacrylamide gel-immobilized cells.

Metal removal is shown for La(III) alone (●), in the presence of Th(IV) (○), Th(IV) alone (■) and in the presence of La(III) (□) at various flow rates as described in Materials and Methods.

Figure 3. Removal of neodymium (●) and europium (■) at various flow rates. Open and filled symbols refer to two independent preparations. The biofilms were tested after 3 months of storage at 4 °C. The $FA_{1/2}$ value is that flow rate giving 50% removal of metal from solution, being (for Nd) 272 and 275 mL/h for two independent preparations.

Figure 4. Accumulation of metal precipitate by biofilm. A: polyurethane foam disc before biofilm formation (inset) and following biofilm growth with Nd-precipitate (main panel). Notable diagnostic purple coloration (not shown). B,D: Biofilm growth on the foam. Note coverage is not complete and is less at the edges of the foam. The biofilm has a typical convoluted surface (C,D). C: Biofilm is shown before (C) and following (D) Nd exposure at the same magnification. Note that metal-unchallenged and metal coated biofilm appears similar at low magnification but at high

magnification single cells have become occluded by precipitate (F) as compared to biofilm without metal (E).

Figure 5. Analysis of neodymium precipitate on the biofilm. A: Co-localization of Nd, P (precipitate) and C and O (bacteria) by EDX mapping. B: Elemental analysis by EDX of a small area of the metal coated biofilm (shown inset). C: X-ray powder diffraction pattern of bulk samples. Top and bottom patterns (pale and dark grey) are from biomaterial made using 3 month old biofilms (from two independent preparations). X-ray powder patterns were identical for material made using a 10 month old biofilm. Vertical lines are database reference lines for NdPO_4 .

Figure 6. Effect of biofilm ageing on removal of Nd(III). Data are pooled from two independent preparations, each normalised to 100% for the $\text{FA}_{1/2}$ value obtained using freshly harvested biofilms. The identical data for two independent 3 month old biofilms are shown as a common point (open symbol). A: Loss of metal accumulation capability with biofilm age. B: Log plot of A shows exponential loss of activity with a biofilm half life of 3 months.

Figure 7. Effect of exposure to pH 3.5 on removal of Nd(III). Biofilms (10-11 months old) were challenged with Nd(III) at pH 5.5 (■) and then at pH 3.5 (●) followed by a return to pH 5.5 (▲) with a minimum of 2 column volumes of wash between each change of pH. Representative data (with $\text{FA}_{1/2}$ values) are shown (see text).

Figures

Figure 1

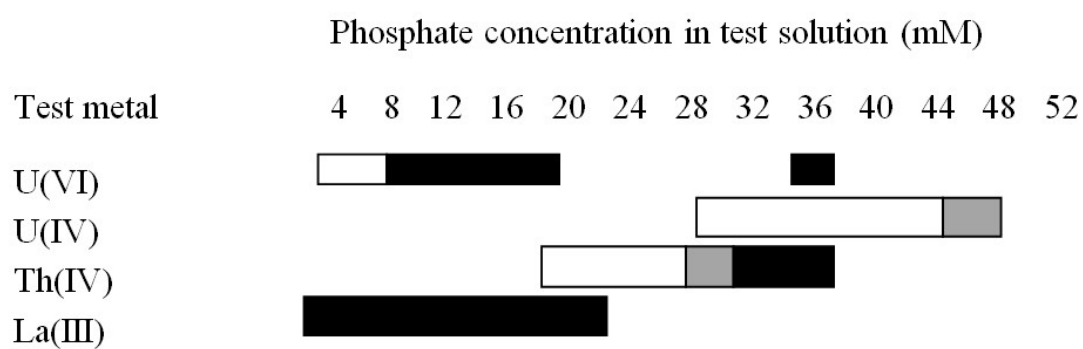


Figure 2

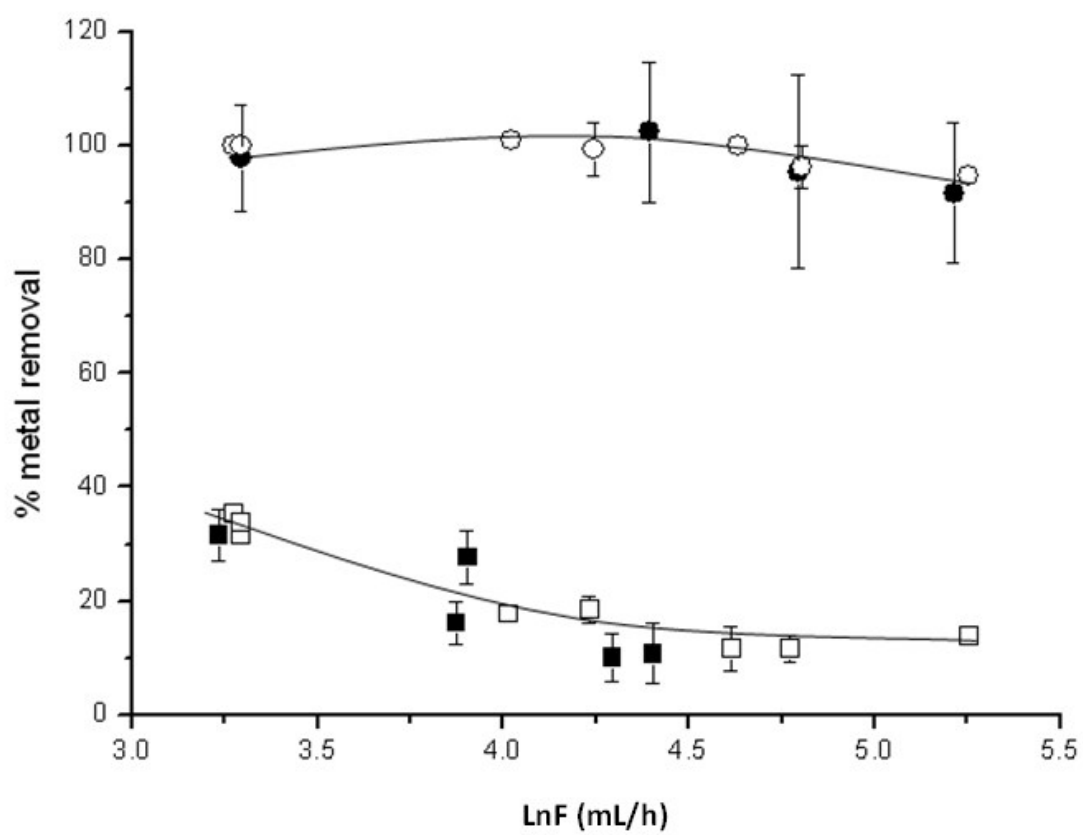


Figure 3

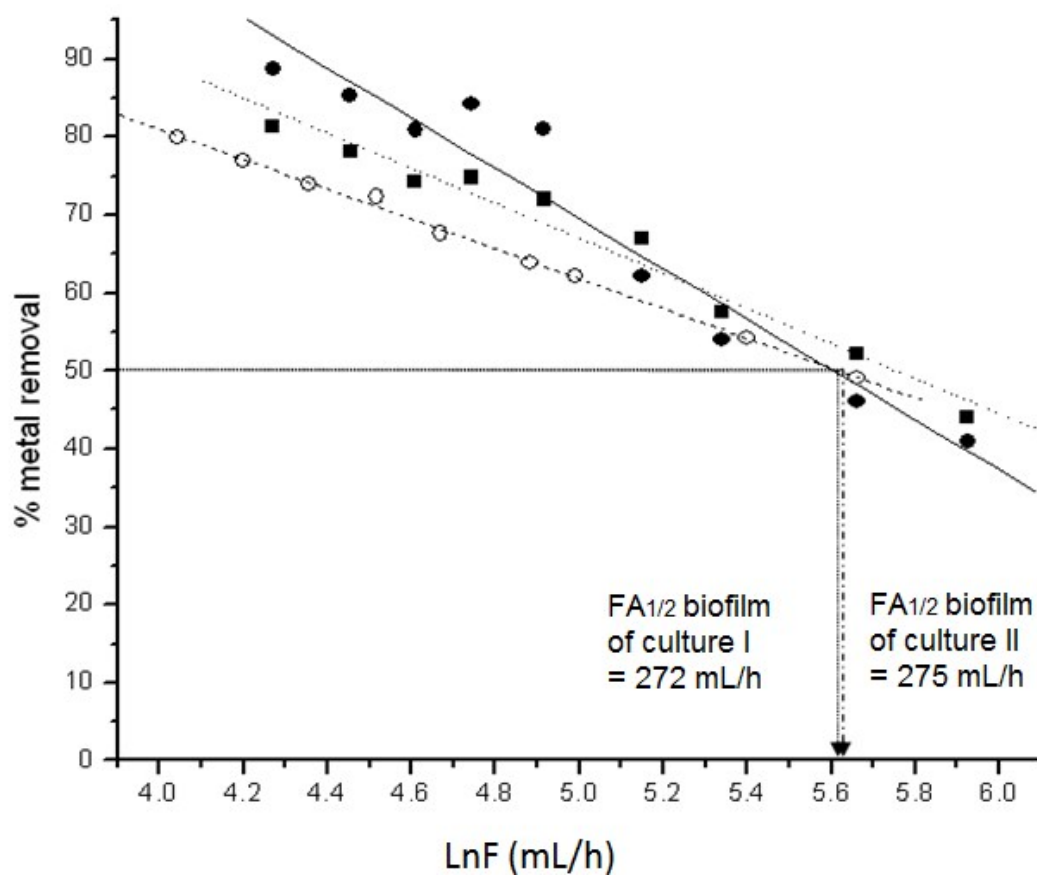


Figure 4

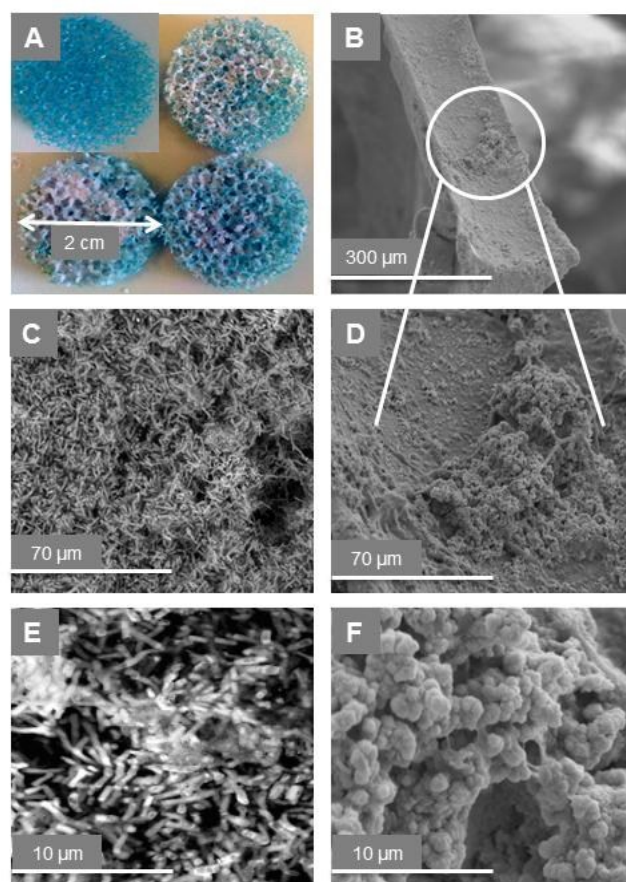


Figure 5

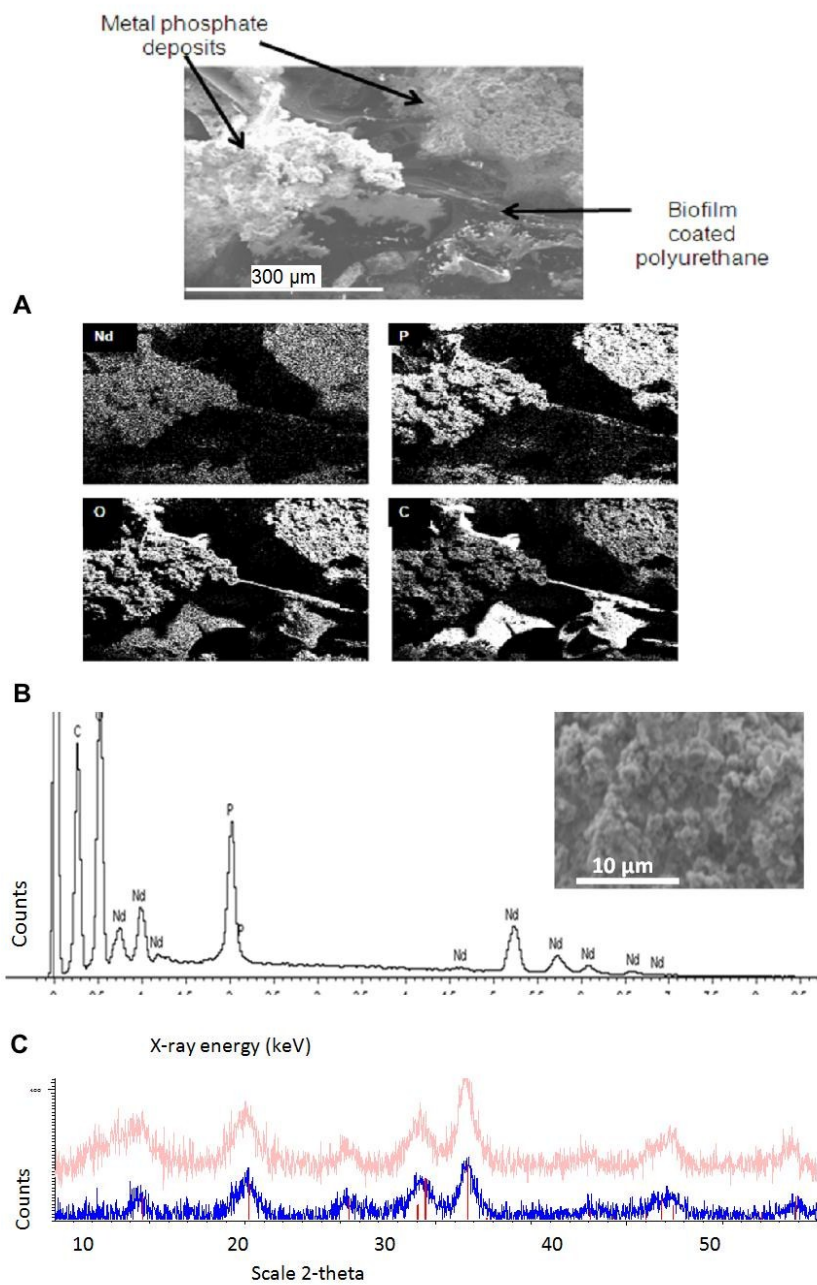
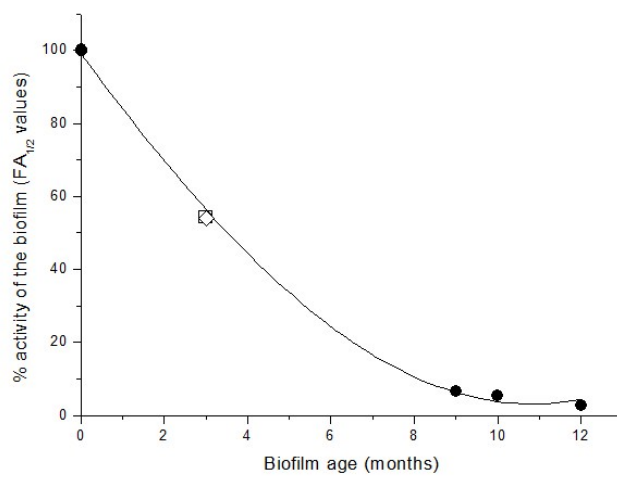


Figure 6

A



B

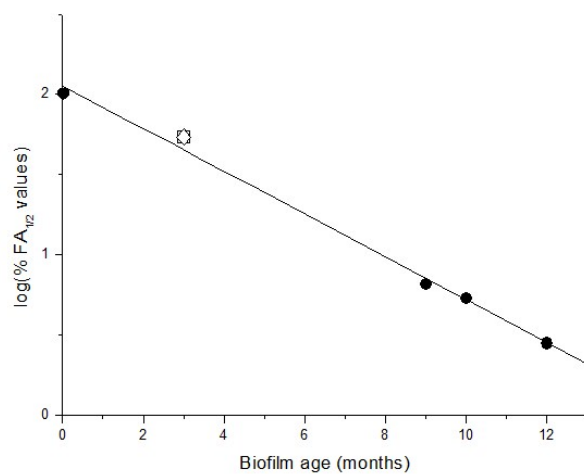


Figure 7

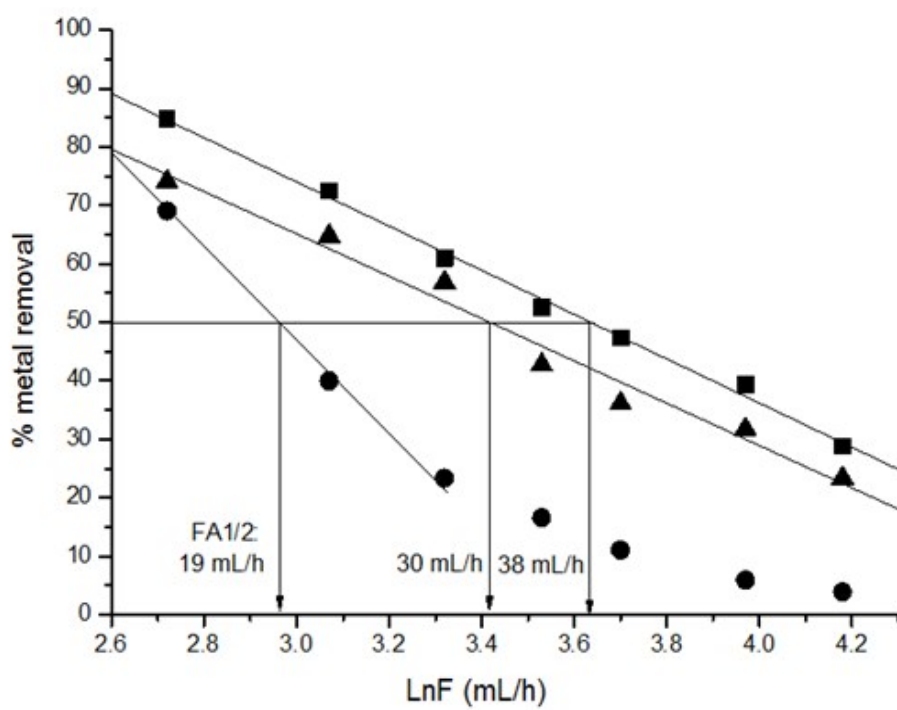




Figure 1. Precipitation of U(VI), U(IV), Th(IV) and La(III) in cell-free test solution. Metals were added as their nitrate salts to the column mixture (to 1 mM) and sodium phosphate solution was added (at the same pH) to the concentration shown (mM). Tubes were mixed and examined after 10 and 30 min for visible precipitate. Black: precipitate visible in 10 min. Grey: precipitate visible in 30 min. White: no precipitate after 30 min.

17x7mm (300 x 300 DPI)

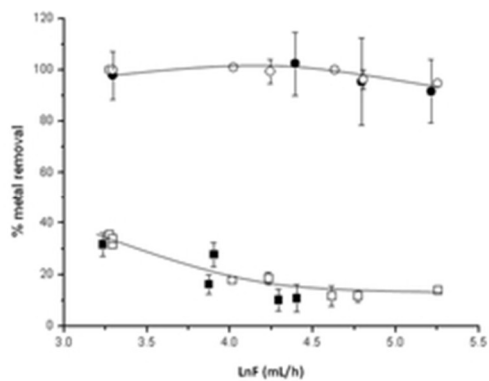


Figure 2. Removal of La(III) and Th(IV) by polyacrylamide gel-immobilized cells. Metal removal is shown for La(III) alone (●), in the presence of Th(IV) (○), Th(IV) alone (■) and in the presence of La(III) (□) at various flow rates as described in Materials and Methods. ●○■□
21x15mm (300 x 300 DPI)

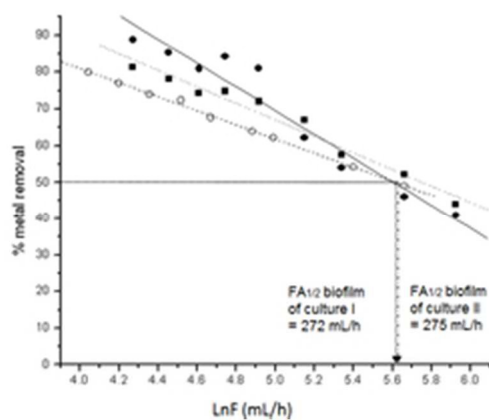


Figure 3. Removal of neodymium (●) and europium (■) at various flow rates. Open and filled symbols refer to two independent preparations. The biofilms were tested after 3 months of storage at 4 oC. The FA1/2 value is that flow rate giving 50% removal of metal from solution, being (for Nd) 272 and 275 mL/h for two independent preparations.
21x17mm (300 x 300 DPI)

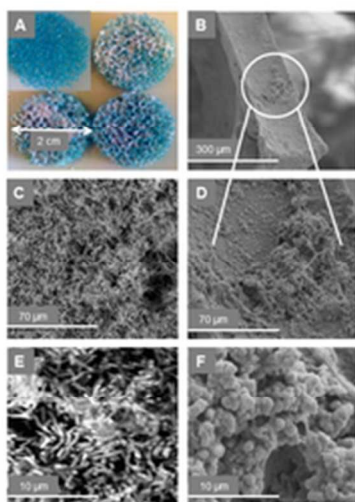


Figure 4. Accumulation of metal precipitate by biofilm. A: polyurethane foam disc before biofilm formation (inset) and following biofilm growth with Nd-precipitate (main panel). Notable diagnostic purple coloration (not shown). B,D: Biofilm growth on the foam. Note coverage is not complete and is less at the edges of the foam. The biofilm has a typical convoluted surface (C,D). C: Biofilm is shown before (C) and following (D) Nd exposure at the same magnification. Note that metal-unchallenged and metal coated biofilm appears similar at low magnification but at high magnification single cells have become occluded by precipitate (F) as compared to biofilm without metal (E).
30x22mm (300 x 300 DPI)

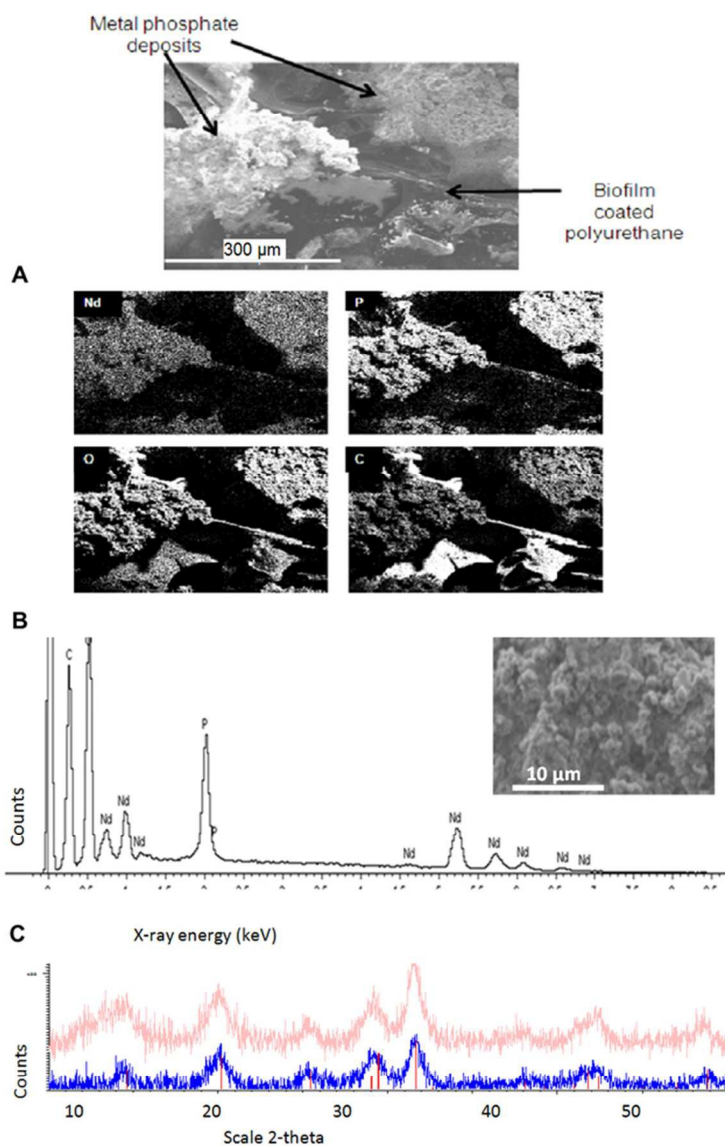


Figure 5. Analysis of neodymium precipitate on the biofilm. A: Co-localization of Nd, P (precipitate) and C and O (bacteria) by EDX mapping. B: Elemental analysis by EDX of a small area of the metal coated biofilm (shown inset). C: X-ray powder diffraction pattern of bulk samples. Top and bottom patterns (pale and dark grey) are from biomaterial made using 3 month old biofilms (from two independent preparations). X-ray powder patterns were identical for material made using a 10 month old biofilm. Vertical lines are database reference lines for NdPO_4 .
58x87mm (300 x 300 DPI)

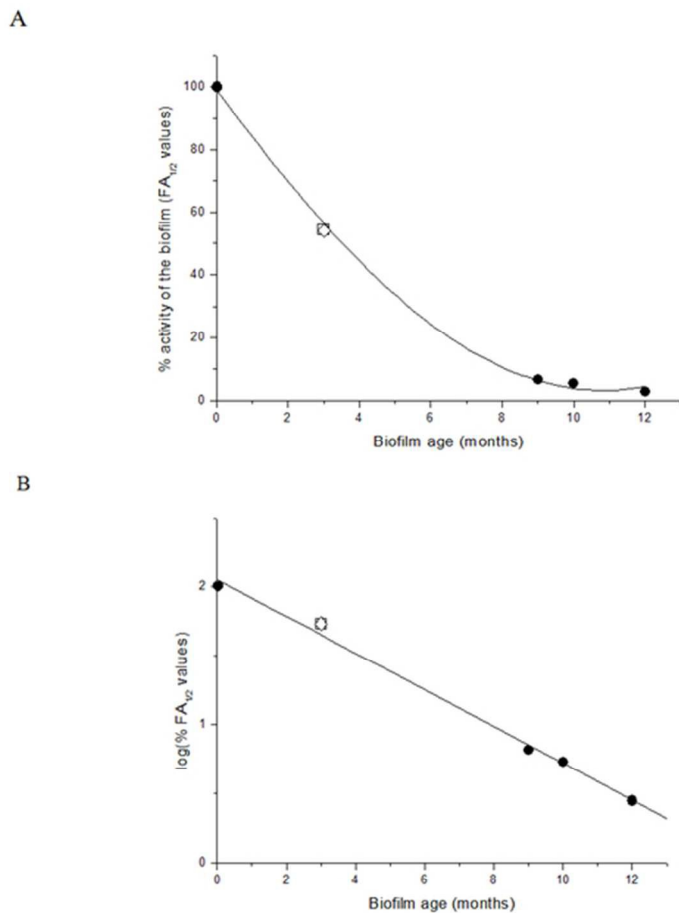


Figure 6. Effect of biofilm ageing on removal of Nd(III). Data are pooled from two independent preparations, each normalised to 100% for the $FA_{1/2}$ value obtained using freshly harvested biofilms. The identical data for two independent 3 month old biofilms are shown as a common point (open symbol). A: Loss of metal accumulation capability with biofilm age. B: Log plot of A shows exponential loss of activity with a biofilm half life of 3 months.
54x69mm (300 x 300 DPI)

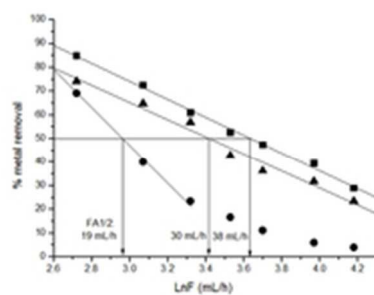


Figure 7. Effect of exposure to pH 3.5 on removal of Nd(III). Biofilms (10-11 months old) were challenged with Nd(III) at pH 5.5 (■) and then at pH 3.5 (●) followed by a return to pH 5.5 (▲) with a minimum of 2 column volumes of wash between each change of pH. Representative data (with FA1/2 values) are shown (see text).

18x13mm (300 x 300 DPI)